

# Femtosecond laser ablation of a metal, a dielectric and a semiconductor illuminated at oblique angles of incidence

Xiao-Long Liu,<sup>1,2</sup> Weibo Cheng,<sup>1</sup> Massimo Petrarca,<sup>3</sup> and Pavel Polynkin<sup>1, a)</sup>

<sup>1)</sup>College of Optical Sciences, University of Arizona, Tucson, AZ 85721, USA

<sup>2)</sup>Academy of Opto-Electronics, Chinese Academy of Science, Beijing 100094, China

<sup>3)</sup>La Sapienza University, SBAI Department, via A. Scarpa 14, 00161 Rome, Italy

We report the measurements of fluence thresholds for single-shot femtosecond laser ablation, as functions of the angle of incidence and at different polarizations of the laser beam, for a metal, a dielectric and a semiconductor. We use the linear index of refraction, unperturbed by the ablating laser pulse, to compute the values of the laser fluence transmitted into the material, corresponding to the measured values of the ablation threshold fluence in the incident beam. Our data show that, in spite of the complex nonlinear ionization dynamics involved in the ablation process, thus computed transmitted threshold fluence is remarkably independent of the angle of incidence and polarization of the laser beam, for all three material types. We suggest that the angular dependence of ablation threshold can be utilized for profiling fluence distributions in ultra-intense femtosecond laser beams.

PACS numbers: 79.20.Eb, 42.25.Bs, 42.60.Jf

Analytical studies of ablation with ultrashort laser pulses are motivated both by applications in micromachining and by the need to understand optical damage by intense femtosecond laser pulses. Virtually all of the prior studies have been conducted for the case when the ablating laser pulse strikes the surface of the material at normal angle of incidence (AOI). However, in practice, many if not most optics are used at oblique AOIs (most commonly at  $45^\circ$  or at the Brewster's angle). In spite of the widespread use of optics with oblique incidence of the laser beam, there have been no systematic study of the dependence of ablation threshold fluence on the AOI for different kinds of materials.

Prior scarce investigations of femtosecond laser ablation and laser damage at not-normal AOIs focused on specific applications. In particular, measurements of the ablation rate dependence on the AOI and polarization for copper have been reported<sup>1</sup>. An effective penetration depth of the laser field into the material, different from the optical penetration depth calculated classically from the value of the complex index of refraction, has been introduced to explain the measured data. Laser ablation thresholds for polyimide films at various AOIs and different polarizations have been quantified<sup>2</sup>. (Polyimide was used as a model material for the corneal tissue.)

In this paper, we report experimental results on the dependence of laser ablation threshold on the AOI and polarization of the incident laser beam, for dissimilar materials including a metal, a dielectric and a semiconductor. We find that at large AOIs and for S-polarization of the incident beam, a metallic surface can be as resistant to optical damage as the surface of a dielectric. We show that the value of the transmitted threshold laser fluence,

calculated as if the reflective and absorptive properties of the material were not affected by the ablating laser pulse, is remarkably independent of the AOI and polarization of the laser beam. We suggest that the dependence of the ablation threshold fluence on the AOI can be used for profiling fluence distributions in ultra-intense laser beams with the peak fluence exceeding the damage threshold fluence of common optical materials.

Our experiments make use of a commercial Ti:Sapphire ultrafast laser system that delivers 60 fs-long pulses with 4 mJ of energy per pulse at the pulse repetition rate of 1 kHz. The optical spectrum of the laser pulses is centered at 800 nm. The energy of the laser pulses used for ablation can be continuously varied by a half-wave plate followed by a reflection off a glass wedge at the Brewster's angle. The orientation of the linear polarization of the laser beam incident on the sample is controlled via another half-wave plate. In our experiments, we investigated the cases of P- and S-polarizations, which correspond to the direction of the electric field vector of the laser beam parallel and perpendicular to the plane of incidence, respectively.

The 9 mm-diameter beam produced by the laser system is apertured down to 4 mm diameter and focused on the sample's surface using a lens with a focal length of 50 mm. We checked by a calculation that the fluence profile of the laser beam, propagating linearly, is very close to Gaussian on the surface of the sample. The resulting  $1/e^2$  beam diameter in the focal plane of the lens is  $18 \mu\text{m}$ . The sample is fixed to a manual rotation stage with the rotational accuracy of  $0.1^\circ$ . The rotation stage is mounted on a computer-controlled motorized linear translation stage with the maximum travel speed of 50 mm/s, thus enabling ablation in the single-shot regime. Care is exercised in aligning the setup so that the front surface of the sample always stays in the focal plane of the focusing lens while the sample is translated by the motorized stage. In

<sup>a)</sup>Electronic mail: ppolynkin@optics.arizona.edu

the range of AOIs that we investigated, the surface of the sample interacting with the focused laser beam is always within the beam's Rayleigh range.

For every particular value of the AOI set by the rotation stage, we produce single-shot ablation marks with increasing values of energy of the ablating laser pulse. Ablation is performed in the ambient air. Example SEM images of the ablation craters, for the case of a gold sample ablated by an S-polarized laser beam with  $6.5 \mu\text{J}$  of energy per pulse, are shown in Figure 1. The sample is a  $1000 \text{ \AA}$ -thick gold layer deposited on a silicon wafer. The ablation craters have sharp and clearly defined boundaries, which indicates that femtosecond laser ablation is a threshold process with respect to the local laser fluence. As expected, the ellipticity of the craters grows as  $\propto 1/\cos(\text{AOI})$ , as the AOI is increased.

In order to deduce the value of the ablation threshold fluence, at a particular AOI, we plot the size of the ablation crater squared (e.g., the diameter of the ablation crater squared for the case of normal incidence), vs. logarithm of the pulse energy. If the fluence distribution of the laser beam on the sample is Gaussian, the data plotted that way show a linear dependence with the slope equal to twice the  $1/e^2$  beam radius squared; the extrapolation of the linear dependence to zero crater size yields the value of the ablation threshold fluence<sup>3</sup>. For the case of an oblique AOI, we separately plot the data for the short and for the long axes of the elliptical ablation craters.

The integrity of the data collected in our experiments implies that the data satisfy the following four conditions: (i) The dependencies of the lengths of the long and of the short axes of the elliptical ablation craters squared, on the logarithm of the pulse energy, are both linear; (ii) the size of the laser beam incident on the sample, extracted from the slope of the data curve for the short axis, is independent of the AOI and equal to the value that is calculated assuming linear focusing of the beam; (iii) the size of the beam extracted from the data for the long axis, multiplied by the cosine of the AOI, is also independent of the AOI and equal to the size of the incident beam; (iv) finally, the values of the ablation threshold fluence obtained from the extrapolations of the data for the long and for the short axes, at a particular AOI, are equal to each other. All the data shown in this paper pass the above integrity checks. Examples of the data obtained with a gold sample illuminated at  $45^\circ$  AOI, for the cases of P- and S-polarizations of the ablating laser beam, are shown in Figure 2.

We point out that these measurements need to be performed at sufficiently low values of the pulse energy, so that the length of the short axis of the elliptical ablation crater does not significantly exceed the FWHM beam size of the incident beam. If the energy is too high and the corresponding length of the short axis significantly exceeds the beam size, the deviations of the spatial beam profile from the Gaussian shape, which are inevitably present at the periphery of the beam, will cause the de-

pendence shown in Figure 2 to become nonlinear, thus increasing the uncertainty of the data extrapolation to the zero crater size. We also point out that the fact that the peak fluence on the beam axis can significantly exceed the ablation threshold value, thus enabling the onset of thermal effects in ablation<sup>4</sup> and material blow-off<sup>5</sup>, is of no importance here, as we are not interested in the appearance of the center of the ablation crater, but only of its boundary, where the local laser fluence always equals the ablation threshold fluence.

Even though our experiments are conducted in air, and air ionization may occur for some of the values of the pulse energy that we use, the generated plasma has negligible effect on the propagation of the laser beam towards the sample, because very tight focusing of the laser beam with the lens (with the corresponding f-number of 12.5) always dominates diffraction on the generated plasma. Accordingly, for all data shown in this paper, the values of the beam diameter extracted from the slopes of the ablation curves, such as the ones shown in Figure 2, are always constant and equal to the value calculated assuming linear propagation of the focused laser beam.

Before proceeding to the discussion of our experimental results, let us ask a question: What dependence of the ablation threshold fluence on the AOI should be anticipated? Generally, the threshold for femtosecond laser ablation is reached when a specific amount of laser energy, per atom or molecule of the material, is absorbed in the top layer of the sample. Therefore, it seems natural to expect that the threshold fluence should increase with the AOI, since the area of the sample, that the laser fluence is spread over, grows as  $\propto 1/\cos(\text{AOI})$ . The rigorously computed value of fluence, absorbed per particle in the top layer of the sample, is, in general, a complex nonlinear function of the incident laser fluence, because both reflective and absorptive properties of the medium are transiently altered by the ablating laser pulse. Therefore it may be unreasonable to expect that the absorbed fluence will simply equal to the incident fluence times the factor  $1/\cos(\text{AOI})$ . In what follows, we will present the data for the ablation threshold fluence together with the corresponding values of the threshold fluence multiplied by the factor  $1/\cos(\text{AOI})$ , as well as the approximate values of the threshold laser fluence transmitted through the top surface of the material. Those values of the transmitted fluence will be calculated using Fresnel formulas with the constant (linear) complex index of refraction, as if the optical properties of the material were not perturbed by the incident laser field. Our results will show that thus calculated internal laser fluence is remarkably independent of both the AOI and polarization of the laser beam for different materials, even though the complex index of refraction of those materials can change significantly within the duration of the ablating laser pulse<sup>6</sup>. We will discuss these findings after presenting our data.

We start with the case of a metal. As in the cases shown in Figure 1 and 2, our sample is a  $1000 \text{ \AA}$ -thick layer of gold deposited on a silicon wafer (surface flat-

ness  $\lambda/10$ ). This film thickness is large enough for the gold layer to respond to the near-infrared femtosecond laser excitation as bulk gold<sup>7</sup>. In Figure 3, we show the data for the ablation threshold fluence, at different AOIs, together with the corresponding values of the threshold fluence multiplied by the factor  $1/\cos$  (AOI) and the corresponding values of the transmitted laser fluence, computed with the unperturbed complex index of refraction of gold  $n = 0.1886 + i \cdot 4.7053$ , at 800 nm wavelength. In calculating the E-field immediately below the gold surface we used the standard Fresnel formulas with a complex refractive index. For the case of a metal, the laser energy transmitted through the material surface is absorbed in the material entirely, therefore in this case the transmitted fluence is equivalent to the absorbed fluence.

It is evident from the data that the ablation threshold fluence weakly depends on the AOI for P-polarization and is a growing function of the AOI for S-polarization. The threshold fluence times  $\cos(\text{AOI})$  is a slightly decreasing function of the AOI for P-polarization and is a growing function of the AOI for S-polarization. However, the value of the approximate internal fluence at the point of ablation threshold is invariant with respect to both the AOI and polarization of the incident laser beam.

The value of the ablation threshold fluence for gold that we measure at normal incidence is  $(0.98 \pm 0.05) \text{ J/cm}^2$ , which is close to the previously reported value<sup>7</sup>. Note that throughout this paper, we show the peak value of the ablation threshold fluence (fluence on the axis of the beam), which is, for a Gaussian beam, by a factor of 2 larger than the average threshold fluence used by many other authors.

The second case we consider is that of a wide-bandgap dielectric material – soda-lime glass. As samples, we use standard microscope slides with the surface flatness of  $\lambda/4$ . Data for the ablation threshold fluence, together with the related quantities, are shown in Figure 3. Here, the threshold fluence is a growing function of the AOI for both polarizations. Also for both polarizations, the threshold fluence multiplied by the cosine of AOI is nearly independent of the AOI. And so is the value of the internal fluence at the point of ablation threshold. The internal fluence just below the material surface is calculated here using a constant, unperturbed by the laser field, index of refraction of  $n = 1.45$ , with a negligibly small imaginary part.

The value of the ablation threshold fluence for soda-lime glass that we measure at normal incidence is  $(2.03 \pm 0.07) \text{ J/cm}^2$ . It is in good agreement with the value reported for the case of ablation of borosilicate glass with 50 fs pulses at 780 nm wavelength<sup>8</sup>.

The third material type we consider is a semiconductor. Here our sample is a commercial, un-doped, single-crystal (100) silicon wafer (the normal to the wafer's polished surface is parallel to the [100] direction in the crystal lattice). To illuminate the sample at an oblique AOI, we tilt it by rotating it around the [011] direction; the plane of incidence for the laser beam is per-

pendicular to that direction. Differently from the cases of gold (polycrystalline) and glass (amorphous), silicon is a single-crystal, anisotropic material. Since silicon has a diamond-cubic crystal-lattice type, its optical properties are the same in all directions. However, the anisotropy of the effective electron mass in silicon may result in the dependence of ionization and ablation on the orientation of the crystal, as was previously shown for the case of multi-shot ablation<sup>9</sup>. The issue of ablation anisotropy that could result from the crystalline nature of silicon is beyond the scope of this paper. In Figure 4, we show the ablation threshold fluence, together with the related quantities, as functions of the AOI, for a (100) silicon wafer. As in the case of soda-lime glass discussed above, the ablation threshold fluence is a growing function of the AOI for both polarizations of the laser beam. The threshold fluence times  $\cos(\text{AOI})$  is also an increasing function of the AOI for both polarizations. However, as in the cases of a metal and a glass, the value of the internal laser fluence at the point of ablation threshold is invariant with respect to the AOI and polarization. Here, the internal fluence is again calculated using a constant (unperturbed by the laser field) value of the complex index of refraction for silicon at 800 nm wavelength,  $n = 3.6959 + i \cdot 0.0047$ .

The value of the ablation threshold fluence for (100) silicon that we measure at normal incidence is  $(0.13 \pm 0.02) \text{ J/cm}^2$ . We are not aware of any previously reported data for thresholds of ablation of (100) silicon with  $\sim 50$  fs laser pulses at 800 nm wavelength.

As pointed out above, the value of the absorbed laser energy per particle, at ablation threshold should be independent of the AOI and polarization. In general, the fluence absorbed in the top layer of the sample is a complex and nonlinear function of the incident laser fluence, as both reflective and absorptive properties of the material are transiently altered by the ablating laser pulse. Our data empirically show that the quantity equal to the transmitted laser fluence, computed as if the reflective properties of the sample were unchanged through the interaction of the sample with the laser pulse, is nearly independent of the AOI and polarization. That observation empirically suggests that thus calculated transmitted fluence and the total energy absorbed in the top layer of the sample, are proportional to each other, and the proportionality coefficient is independent of the AOI and polarization. For the case of gold, such an observation is expected, as the reflective and absorptive properties of gold weakly change during the interaction. For the cases of glass and silicon, we argue that the transmission of the incident laser energy into the sample decreases, while absorption in the top layer of the sample increases, as the sample is ionized by the laser pulse. Our data empirically show that the two effects somewhat compensate each other.

A known dependence of the ablation threshold fluence on the AOI can be used for the measurements of the transverse fluence distributions in ultra-intense laser beams, such as femtosecond beams propagating in air in

the self-channeling (filamentation) regime<sup>10</sup>. To profile an intense laser beam, a material that has a quantified strong dependence of the ablation threshold fluence on the AOI needs to be used. We would produce single-shot ablations of that material, at different AOIs, with the beam that has the unknown fluence distribution we wish to quantify. The resulting elliptical ablation patterns would be scaled through the compression along the long axis of the ellipse by the  $\cos(\text{AOI})$  factor. The boundaries of the resulting scaled patterns will outline the slices of the beam profile at different levels of fluence, equal to the values of the ablation threshold fluence at the AOIs used in these beam-profiling experiments. Note that such a profiling procedure does not assume any particular beam shape or axial symmetry.

For example, the data for gold illuminated with S-polarized light shown in Figure 5 suggest that gold can be used for profiling intense laser beams in the range of fluences from 1 to 9 J/cm<sup>2</sup>. For 50 fs FWHM pulse duration, that range of fluences corresponds to the range of peak powers from 20 to 170 TW/cm<sup>2</sup>.

Complex temporal pulse dynamics that may accompany highly nonlinear propagation of ultra-intense laser beams in air<sup>11</sup> will not have a significant effect on the accuracy of the fluence (not intensity) profiling through the procedure discussed above, because the value of ablation threshold fluence is weakly dependent on pulse duration, as long as the pulse is shorter than few hundred femtoseconds but longer than  $\sim 30$  fs<sup>7,12</sup>. The ultra-short temporal spikes that may develop in the intensity profile of the laser pulse will also not significantly affect the accuracy of the fluence profiling because those spikes carry only a small fraction of the overall fluence of the laser beam.

In conclusion, we have experimentally investigated the dependence of the threshold fluence for single-shot femtosecond laser ablation on the angle of incidence and polarization of the ablating laser beam. We have found that for optically dissimilar materials (metal, glass, semi-

conductor), the value of the fluence transmitted into the material at the point of ablation threshold, if calculated using the linear (unperturbed by the laser field) value of the complex index of refraction, is nearly independent on the angle of incidence and polarization. These findings suggest that ablation is driven by the fluence or by the electric field of the ablating laser pulse immediately below the material surface. The dependence of the ablation threshold fluence on the angle of incidence can be utilized for profiling fluence distributions in ultra-intense laser beams in the range from a fraction of 1 J/cm<sup>2</sup> up to about 10 J/cm<sup>2</sup>.

We thank Mr. Lee Johnson and Prof. Thomas Milster for the assistance with operating the electron microscope. This work was supported by the US Defense Threat Reduction Agency under program HDTRA 1-14-1-0009 and by the United States Air Force Office of Scientific Research under programs FA9550-12-1-0482 and FA9550-16-1-0013. X.-L. Liu acknowledges the support from the National Natural Science Foundation of China through grants No. 11404335 and No. 91538113.

- <sup>1</sup>Y. Miyasaka, M. Hashida, T. Nishii, S. Inoue, S. Sakabe, *Appl. Phys. Lett.* **106**, 013101 (2015).
- <sup>2</sup>B. S. Haq, H. U. Khan, K. Alam, M. Mateenullah, S. Attaullah, I. Zari, *Appl. Opt.* **54**, 7413 (2015).
- <sup>3</sup>J. M. Liu, *Opt. Lett.* **7**, 196 (1982).
- <sup>4</sup>S. Nolte, C. Momma, H. Jackobs, A. Tünnermann, B. N. Chichkov, B. Wellegehausen, H. Welling, *J. Opt. Soc. Am. B* **2716** (1997).
- <sup>5</sup>D. Bouilly, D. Perez, L. J. Lewis, *Phys. Rev. B* **76**, 184119 (2007).
- <sup>6</sup>K. Sokolowski-Tinten, J. Bialkowski, M. Boing, A. Cavalleri, D. von der Linde, *Phys. Rev. B* **58**, R11805 (1998).
- <sup>7</sup>B. Stewart, M. Feit, S. Herman, A. Rubenchik, B. Shore, M. Perry, *J. Opt. Soc. Am. B* **13**, 459 (1996).
- <sup>8</sup>W. Kautek, J. Krüger, M. Lenzner, S. Sartania, C. Spielmann, F. Krausz, *Appl. Phys. Lett.* **69**, 3146 (1996).
- <sup>9</sup>X. Li, W. Rong, L. Jiang, K. Zhang, C. Li, Q. Cao, G. Zhang, Y. Lu, *Opt. Exp.* **22**, 30170 (2014).
- <sup>10</sup>A. Couairon, A. Mysyrowicz, *Phys. Rep.* **441**, 47 (2007).
- <sup>11</sup>M. Gaarde, A. Couairon, *Phys. Rev. Lett.* **103**, 043901 (2009).
- <sup>12</sup>B. Chimier, O. Utéza, N. Sanner, M. Sentis, T. Itina, P. Lassonde, F. Légaré, F. Vidal, J. C. Kieffer, *Phys. Rev. B* **84**, 094104 (2011).

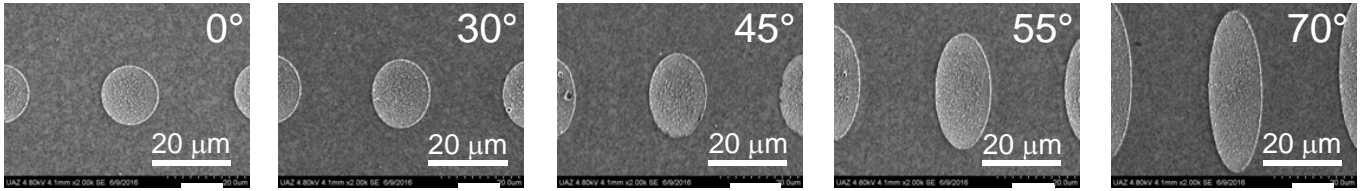


FIG. 1. SEM images of single-shot ablation craters produced on a gold surface by an S-polarized, 60 fs-long laser pulse with  $6.5 \mu\text{J}$  of energy at 800 nm wavelength, at different angles of incidence, as indicated in the individual images.

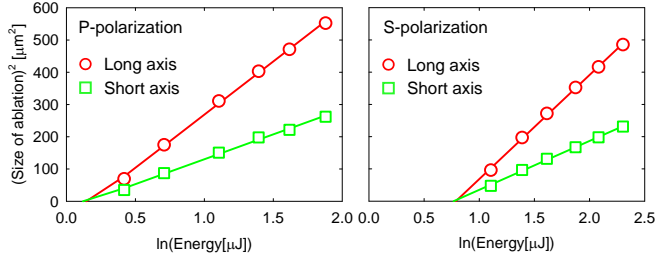


FIG. 2. Examples of the data for the size of the ablation crater squared vs. logarithm of the energy of the ablating laser pulse, for the case of a gold sample illuminated at  $45^\circ$  AOI. The left and right panels are for the cases of P- and S-polarizations of the incident laser beam, respectively. The two lines of data on each plot correspond to the long and short axes of the elliptical ablation crater. The experimental errors in these data are small compared to the size of the data symbols.

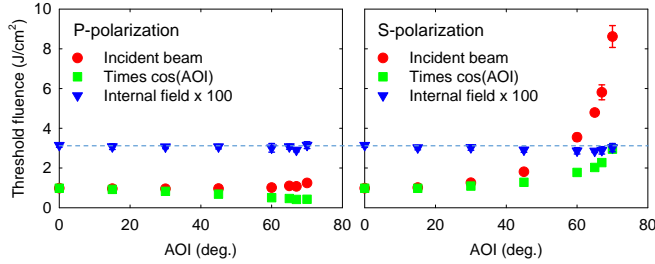


FIG. 3. Ablation threshold fluence and the quantities related to it, vs. the AOI of the laser beam on the gold sample. The value of the internal fluence shown is multiplied by a factor of 100, to make it visible on the plots. The experimental errors are due to the extrapolation uncertainty at large values of the AOI.

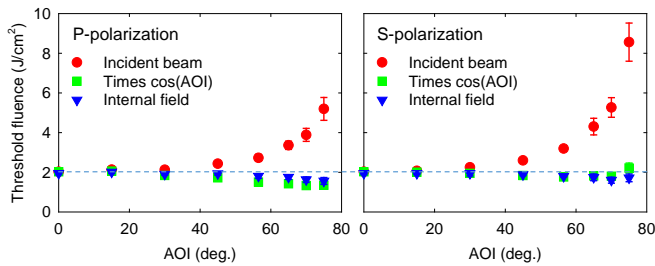


FIG. 4. Same as in Figure 3, but for the case of soda-lime glass.

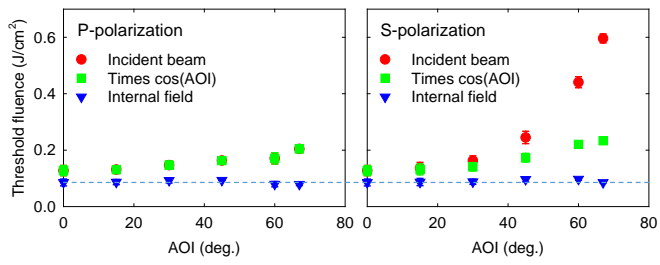


FIG. 5. Same as in Figures 3 and 4 but for the case of (100) silicon.